



3 1176 00166 4540

NASA CR-163113

NASA Contractor Report 163113

NASA-CR-163113
1981 00 20556

DRAG REDUCTION OBTAINED BY THE ADDITION OF A
BOATTAIL TO A BOX SHAPED VEHICLE

Randall L. Peterson

August 1981

LIBRARY COPY

AUG 27 1981

163113 LIBRARY CENTER
LIBRARY, NASA
JOHNSON SPACE CENTER

NASA

NF02064

NASA Contractor Report 163113

DRAG REDUCTION OBTAINED BY THE ADDITION OF A
BOATTAIL TO A BOX SHAPED VEHICLE

Randall L. Peterson
California Polytechnic State University
San Luis Obispo, California

Prepared for
Dryden Flight Research Center
under Contract NCC 4-1

NASA
National Aeronautics and
Space Administration
1981

Intentionally Left Blank

TABLE OF CONTENTS

	Page
TABLE OF CONTENTS.....	iii
LIST OF SYMBOLS.....	iv
LIST OF FIGURES.....	v
LIST OF TABLES.....	vii
ACKNOWLEDGEMENTS.....	viii
INTRODUCTION.....	1
TEST VEHICLE.....	1
EXPERIMENTAL CONCEPT.....	3
METHOD AND INSTRUMENTATION.....	4
TEST CONDITIONS.....	5
RESULTS AND DISCUSSION.....	5
Flow Visualization.....	5
Aerodynamic Drag.....	6
CONCLUDING REMARKS.....	7
REFERENCES.....	8
FIGURES AND TABLES.....	9

LIST OF SYMBOLS

<i>a</i>	vehicle acceleration
<i>A</i>	body cross-sectional reference area, 3.3 m^2 (35.3 ft^2)
<i>A'</i>	projected cross-sectional reference area used in reference 5 for a 1/10 scale model, based on body plus wheels, at same scale $A' = 1.053 A$
C_{D_a}	aerodynamic drag coefficient, D_a/qA
D_a	aerodynamic drag
D_e	equivalent diameter, $\sqrt{4A/\pi}$
D_m	mechanical drag
<i>f</i>	rolling resistance coefficient
<i>g</i>	local acceleration due to gravity, 9.795 m/sec^2 (32.137 ft/sec^2)
<i>l</i>	vehicle length
<i>m</i>	vehicle mass, W/g
\bar{m}	effective vehicle mass
Δm	additive mass accounting for rotational inertia
<i>p</i>	tire pressure
<i>q</i>	dynamic pressure, $0.5\rho V^2$
<i>R</i>	Reynolds number based on vehicle length, $\rho V l / \mu$
<i>t</i>	time
<i>V</i>	vehicle velocity
<i>V_o</i>	initial vehicle velocity at <i>t</i> = 0
<i>W</i>	vehicle weight
μ	absolute viscosity
ρ	air density

LIST OF FIGURES

Figure		Page
1	Dimensions of original square-cornered configuration in meters (inches) Reference 1.	9
2	Configuration I, $V = 0$ (engine cooling door closed).....	10
3	Configuration II, vehicle in motion.....	10
4	Configuration III, $V = 0$ (engine cooling door open).....	10
5	Boattail dimensions.....	11
6	Right front wheel well seal as viewed from slightly ahead of wheel station.....	12
7	Sealed underbody as viewed from the front	12
8	Right rear wheel well seal as viewed from slightly ahead of axle.....	12
9	Variation of mechanical drag with vehicle velocity.....	13
10	Fifth-wheel and fifth-wheel support system "side mounting" (configuration I).....	14
11	Fifth-wheel in aft mounting or trailing location (configuration I).....	14
12	Variation of aerodynamic drag with vehicle velocity for the different fifth-wheel mounting locations (configuration I)....	15
13	Instrumentation layout.....	16
14	Tuft patterns for full boattail, configuration II, $V = 116.7 \text{ km/h}$ (72.5 mph).....	17
15	Tuft patterns for full boattail, configuration II, $V = 116.7 \text{ km/h}$ (72.5 mph).....	17
16	Tuft patterns for truncated boattail, configuration III, $V = 107.8 \text{ km/h}$ (67 mph).....	18
17	Tuft patterns for truncated boattail, configuration III, $V = 107.8 \text{ km/h}$ (67 mph).....	18

Figure		Page
18	Variation of aerodynamic drag with vehicle velocity.....	19
	(a) Configuration I, blunt base.....	19
	(b) Configuration II, full boattail.....	20
	(c) Configuration III, truncated boattail.....	21
19	Aerodynamic drag variation with vehicle velocity for all configurations.....	22

LIST OF TABLES

Table	Page
I Comparison of tests run at the Dryden Flight Research Center and the University of Kansas	23

ACKNOWLEDGEMENTS

The advice and comments of Edwin Saltzman of the Dryden Flight Research Center are gratefully acknowledged. The contributions of many others at DFRC are also acknowledged, especially Ken Iliff and Rich Maine of the Dynamics Branch, Lee Adelsbach of the Avionics Branch, Jeff Coonrod of the Fabrication and Repair Branch and Vern Wemple of Automotive Maintenance.

The cooperation of several Edwards Air Force Base organizations was also important to the successful completion of this experiment, and their efforts are also gratefully acknowledged. These organizations are: the Base Operations Branch, the Traffic Management Branch and Detachment 21 of the 2nd Weather Squadron (MAC).

I would also like to thank Dr. John D. Nicolaides, my thesis advisor, for the invaluable assistance that he gave on this project. The NASA Dryden Flight Research Center and the California Polytechnic State University have participated jointly in a graduate student program funded by NASA under Grant NCC 4-1. The Cal Poly program director is Dr. Doral R. Sandlin. This work was supported by the graduate student grant. I would like to thank both Cal Poly and DFRC for the opportunity to participate in this unique and rewarding program.

INTRODUCTION

Due to the continuing increase in fuel prices and the uncertainty of future supplies, a widespread interest in the efficiency of ground vehicles has developed. Of significant interest are improvements in the aerodynamic efficiency of high volume, "box-shaped" transports, such as delivery vans, motor homes, and trucks. This is because the generally poor aerodynamic shape of these vehicles has so much potential for significant improvement in efficiency.

Prior to the fuel crisis and the rise in fuel prices in 1973 very little was done by the manufacturers of ground vehicles to improve the aerodynamic efficiency. Before that time the high aerodynamic drag of box-shaped transports was overcome by using more powerful engines resulting in increases in fuel consumption. After the fuel crisis numerous drag experiments were conducted on full-scale vehicles and wind-tunnel models to improve aerodynamic efficiency.

In 1973 the NASA Dryden Flight Research Center (DFRC) began full-scale tests on a box-shaped van¹. Various combinations of rounded and square corners were tested. Also tested was a faired and sealed underbody². A 52-percent reduction in drag was obtained by rounding the front corners and a 15-percent reduction in drag was achieved by the addition of a full-length underbody seal to configuration C of reference 2. Further ground vehicle experimentation at DFRC included add-on drag reduction devices for tractor-trailer combination trucks^{3,4}.

The present study is a continuation of the tests conducted on the box-shaped vehicle in 1973. The intent of the present experiment is to define a near optimum value of drag coefficient for a high volume type of vehicle through the use of a boattail, on a vehicle already having rounded front corners and an underbody seal, or fairing. The results of these tests will constitute a baseline for later follow-on studies to evaluate candidate methods of obtaining afterbody drag coefficients approaching the boattail values, but without resorting to such impractical afterbody extensions.

The current modifications to the box-shaped vehicle consisted of a full and truncated boattail in conjunction with the faired and sealed underbody. Drag results from these configurations are compared with corresponding wind-tunnel results of a 1/10 scale model.

Test velocities ranged up to 96.6 km/h (60 mph) and the corresponding Reynolds numbers ranged up to 1.3×10^7 based on the vehicles length which includes the boattail. A simple coast-down technique was used to define drag

TEST VEHICLE

The box-shaped test vehicle used in references 1 and 2 was again modified

for the present series of drag reduction studies. The various configurations were achieved as before by relatively simple changes to the sheet metal and subframe. The dimensions of the original square cornered configuration, as reported in references 1, 2 and 4, are shown in figure 1

The three configurations investigated in this study were achieved through the addition of a full-boattail and a truncated-boattail, configurations II and III respectively, to the baseline box-shaped vehicle, configuration I. Configuration I, which had the same overall length, width and height as the square cornered vehicle shown in figure 1, featured rounded forebody horizontal and vertical corners, a faired and sealed underbody and a blunt aft-end, figure 2. This configuration was used as a baseline, for the present tests, to determine the percent decrease in drag obtained by the addition of the full and truncated boattails. Configuration II consisted of the rounded forebody, the faired and sealed underbody and the full boattail, figure 3. The final configuration, configuration III, consisted of the truncated boattail in conjunction with the same rounded forebody and faired and sealed underbody, figure 4

The size and contour of the boattail used in this study was determined from somewhat arbitrarily conceived full-scale size limitations, full-scale (DFRC) tuft studies, and wind-tunnel flow visualization studies on a 1/10 scale model (University of Kansas, reference 5). The length of the boattail from its base to its apex was, for practical considerations, restricted to the width of the test vehicle. This length also approximates the equivalent diameter of the vehicle, D_e . The model flow visualization studies, using tufts and neutrally buoyant helium bubbles to trace the streamlines, showed that the arbitrarily derived boattail geometry was effective in "closing" the flow to produce a relatively small wake.

The full-scale truncated boattail configuration was a direct result of the model flow visualization studies. The length of the truncated boattail was determined by cutting off the portion of the boattail behind the flow separation station as defined by the model tuft results. Dimensions of the full and truncated boattails are presented in figure 5

The full-length underbody seal on the test vehicle was configured so that it faired smoothly into the rounded front lower horizontal surface and the bottom quarter of the boattail. An aft facing gap underneath the vehicle permitted the cooling air that passed through the engine radiator to escape during "cooling-vent-open" operation. The aft part of this gap is shown in the lower left portion of figure 6, immediately below the rear portion of the wheel well. Figure 7 shows the full-length underbody seal as viewed from the front.

The front wheel wells were sealed using tape and fiberglass cloth impregnated with silicone rubber to allow the front suspension system to flex. Figure 6 shows the right front wheel well seal as viewed from a point slightly forward of the right front wheel

The rear wheel wells were sealed using sheet metal and tape. Vertical slots were provided in the rear wheel seals to allow the rear axle to respond

to small road discontinuities without damaging the seals. Figure 8 shows the right rear wheel seal as viewed from a point slightly forward of the rear axle.

EXPERIMENTAL CONCEPT

The equation of motion for a decelerating vehicle is obtained from Newton's second law. The resulting equation of motion is:

$$\bar{m}a = -0.5\rho V^2 C_{D_a} A - f_W$$

The term on the left-hand side of the equation is the effective mass times the acceleration. The first term on the right-hand side is the aerodynamic drag force, and the second term is the mechanical drag force.

The aerodynamic drag force is assumed to be a function of velocity squared, where the aerodynamic drag coefficient (C_{D_a}) is virtually independent of

velocity. The mechanical drag consists of the tractive drag of the tires, bearings and seals, the gear resistance of the differential and drive train and the thrust due to the rotational inertia of the wheels and tires.

Because the mechanical drag was essentially independent of configuration and because of the large number of variables involved, an analytical description of the mechanical drag is considered to be outside the scope of this study. Therefore, the tractive drag, with the tires being the major source, was approximated using a measured rolling resistance at very low velocity in conjunction with Hoerner's equation for rolling resistance⁶.

The second part of the mechanical "drag" is due to the rotational kinetic energy of the tires and wheels. The thrust due to the rotational inertia of the tires and wheels is taken into account in the correction of the vehicles mass. The effective mass of the vehicle is then \bar{m} , where $m = m + \Delta m$ and Δm is the correction for rotational inertia. For this analysis the Δm value used to account for the rotational inertia, as determined from torsional pendulum tests of the tires and wheels, is 2.4-percent of the vehicles mass or $\bar{m} = 1.024$ times the actual mass, m .

To analyze the coast-down data a computer program was written to determine the aerodynamic drag coefficients. This program utilized a finite difference algorithm from the International Math and Statistics Library to find the minimum of the sum of squares of M functions in N variables. The velocity-time data obtained from the coast-down tests were used as residuals in this program from which the minimum aerodynamic drag coefficient was determined. Methods of analyzing coast-down data which have been used by other investigators are presented in references 7 to 10.

METHOD AND INSTRUMENTATION

Coast-down tests are used to experimentally determine the rolling resistance and the aerodynamic drag of road vehicles. This technique has been demonstrated to be a practical method for obtaining high quality drag data for road vehicles under a simulation of actual operating conditions, provided that sufficient care is taken in the details of the test technique. This technique is attractive because of its simplicity and low cost. It also permits data to be obtained at any desired velocity range and in both directions on the test surface.

The coast-down technique consists of accelerating the vehicle to a few miles-per-hour above the starting velocity of each test whereupon the manual transmission is disengaged to allow the vehicle to decelerate in neutral. The time it takes for the vehicle to slow to given velocities is then recorded and used to calculate the vehicle drag. The vehicle was weighed, with occupants, before and after each series of tests to provide the proper mass for computing drag (a "series of tests" is meant herein to refer to the test runs accomplished during a given day).

The mechanical drag of the test vehicle was measured experimentally at very low velocities after each series of tests. This was done by slowly towing the vehicle over a level surface using a hand held spring scale. The measured force was then used as an endpoint in the extrapolation of Hoerner's rolling resistance equation. This extrapolation was assumed to account for the entire mechanical resistance of the test vehicle while decelerating in neutral. The vehicle began each day of testing with a tire pressure of 2.48×10^5 pascals (36 lb/in²). Figure 9 shows the final approximation of mechanical drag as a function of velocity.

All of the drag data for the box-shaped vehicle were obtained during cooling-vent-closed operation. This was done so that the effect of the cooling drag could be eliminated during each coast-down run. The cooling vent was opened between runs and during vehicle acceleration so that overheating of the engine would not occur. A portion of the cooling vent door may be seen at the extreme front of the vehicle in figure 4 whereas, in contrast, the vent was closed in figure 2.

The final drag results for the full and truncated boattail configurations were obtained by subtracting the incremental drag of the fifth-wheel and the fifth-wheel support system (figure 10) from the measured overall drag values containing the "side-mounting" drag increment. The blunt aft-end, baseline configuration was used to determine this increment as it had a fifth-wheel mount located on the blunt aft-end of the vehicle (figure 11), which was not usable in the full and truncated boattail configurations. The incremental drag of the "side-mounted" fifth-wheel and support system was determined by subtracting the coast-down results obtained with the trailing fifth-wheel, on configuration I, from the "side-mounted" coast-down results, also obtained from configuration I. Figure 12 shows these data over the range of test velocities.

All of the drag data for the box-shaped vehicle were obtained using the coast-down technique. The deceleration of the vehicle was measured using a bank of five 0.1-second stopwatches and the calibrated, fifth-wheel driven, precision speedometer which provided a 0.1-mile per hour readout capability. The time increments corresponding to preselected velocity intervals in miles per hour (i.e., 60 to 55, 55 to 50, 50 to 45, 45 to 40, and 40 to 35) were obtained by starting all the stopwatches simultaneously at the starting velocity and stopping them individually at the end of each preselected velocity interval. All of the stopwatch data were hand recorded at the end of each test run. Figure 13 shows the layout of the instrumentation in the vehicle.

TEST CONDITIONS

All of the coast-down tests were made on an auxiliary runway at Edwards Air Force Base, CA. This runway had an exceptionally smooth asphalt surface and a constant elevation gradient of 0.08-percent. The gradient effects on the deceleration were small and were essentially eliminated by the averaging of successive runs in opposite directions. The averaging of successive runs in opposite directions also accounted for head or tail wind effects provided wind conditions remained constant over the duration of both runs. It should be emphasized, however, that test runs were always made early in the day when it was quite calm which virtually eliminated wind effects on the vast majority of test runs.

Wind velocity and direction, ambient pressure and temperature were recorded every 15 minutes at the Edwards Air Force Base weather station during each days series of tests so that the air density could be calculated and general atmospheric factors could be taken into account. The test vehicle was driven to and from the auxiliary runway, a distance of approximately 15.3 kilometers (9.5 miles). This provided a pretest warm-up which also brought the temperature of the oil in the differential up to an essentially steady-state level, thus minimizing the variation of this effect from test-run to test-run.

RESULTS AND DISCUSSION

Flow Visualization

Tuft patterns for the full boattail configuration (configuration II) at a speed of 116.7 km/h (72.5 mph) are shown in figures 14 and 15. Both figures show that the flow separates at or slightly aft of the horizontal and vertical tape lines nearest the apex of the boattail. Figure 14 clearly shows that the flow remains attached over the bottom quarter of the boattail up to this tape line. The achievement of attached flow over the bottom surface of the boattail was considered to be an important factor relative to the overall objectives of

this experiment, i.e., determining a near optimum level of drag for a high volume transport type vehicle through the use of a boattail.

Tuft patterns for the truncated boattail configuration (configuration III) at a speed of 107.8 km/h (67 mph) are shown in figures 16 and 17. Figure 16 clearly shows the attached flow over the top, the bottom and the left side of the truncated boattail. The dangling white tufts in figure 16 show the stagnant conditions that one would expect on a blunt base moving perpendicular to the airflow. Figure 17 shows a more comprehensive view of the attached airflow over the wetted surfaces of the vehicle and the stagnant conditions over the base of the truncated boattail.

Aerodynamic Drag

The aerodynamic drag is presented in figure 18 for each configuration as a function of velocity. The curve for each configuration is a fairing of the coast-down results using a least squares polynomial regression analysis. The curves for all three configurations are presented for comparison purposes on the composite plot in figure 19.

Aerodynamic drag coefficients for each configuration as obtained from the present full-scale tests (DFRC) and corresponding wind-tunnel tests (KU) are summarized in Table I. The full-scale configuration results are for vehicle speeds of 96.6 km/h (60 mph) and 80.5 km/h (50 mph), which for the purposes of this report are considered to be "highway speeds". All of these data are for the cooling vent closed condition so that a more meaningful comparison can be made with the wind-tunnel model results.

The percentage reduction in drag coefficient for both the full-scale tests and the corresponding wind-tunnel tests were obtained by dividing the incremental drag coefficient by the appropriate baseline value. The percentage difference between the wind-tunnel drag coefficient and the full-scale average drag coefficient for each configuration was obtained by dividing their difference by the full-scale average value.

The results given in the table indicate that an average 32-percent reduction in aerodynamic drag was attained with the addition of the full boattail to the blunt aft-end, baseline configuration, at vehicle speeds from 80.5 km/h (50 mph) to 96.6 km/h (60 mph), i.e., highway speeds. The corresponding wind-tunnel results indicated that a 37-percent reduction in aerodynamic drag was attained on the 1/10 scale model at a Reynolds number of 2.7×10^6 . The table also indicates that an average reduction of 31-percent in aerodynamic drag was attained with the truncated boattail on the full-scale vehicle over the same range of highway speeds while corresponding wind-tunnel results showed a 38-percent reduction in aerodynamic drag. The incremental drag coefficient of the side-mounted fifth-wheel and the fifth-wheel support system was determined to be 0.030 ($\Delta C_D = 0.030$) at a vehicle speed of 96.6 km/h (60 mph).

The relatively small difference in drag between configurations II and III (for $V = 96.6 \text{ km/h}$ (60 mph)) indicates that the boattail was cut in approximately the right place. This small drag increment, approximately 3.8-percent at this velocity, shows that it is possible to eliminate the additional length and ineffectual volume of the boattail apex while retaining almost all of the aerodynamic effectiveness of the complete boattail. At a speed of 80.5 km/h (50 mph) or lower, the drag coefficients of configurations II and III are essentially the same, thus establishing the truncated boattail as, overall, the most efficient of the two on the basis of aerodynamic drag and useful volume.

The drag reductions provided by the boattails in the present experiment and in reference 5 are very significant, but they should be interpreted with caution. As was mentioned on pages 5 and 6, "the achievement of attached flow over the bottom surface of the boattail was considered to be an important factor relative to the overall objectives of this experiment, i.e., determining a near optimum level of drag for a high volume transport type vehicle through the use of a boattail." That is to say, providing attached flow upstream of all boattail surfaces is necessary in order to maximize the reduction in afterbody drag. Thus, the rounded forebody corners and the smooth, sealed underbody of the baseline vehicle, configuration I, provided a near ideal candidate vehicle for demonstrating good boattail performance. The reader is hereby forewarned that the addition of a boattail to a configuration having separated flow, or perhaps even relatively low energy flow, over one or more upstream surfaces may result in significantly smaller drag reductions than demonstrated herein or in reference 5 (see references 11 and 12 for examples).

CONCLUDING REMARKS

The effectiveness of the full boattail in delaying flow separation over the aft-end of the vehicle (reducing the size of the wake) is apparent in the average 32-percent reduction in aerodynamic drag, as compared to the baseline drag, at highway speeds. The relative effectiveness of the truncated boattail is similarly apparent in the average 31-percent reduction in aerodynamic drag as compared to the baseline configuration.

The small drag increase, approximately 3.8-percent at 96.6 km/h (60 mph), which occurred when the boattail was truncated indicates that the boattail was cut in approximately the right place. This relatively small increase in drag shows that it is possible to eliminate the additional length and ineffectual volume of the boattail apex while retaining almost all of the aerodynamic effectiveness of the full boattail. The drag coefficients of the full and truncated boattails are essentially the same for speeds of 80.5 km/h (50 mph) and lower. Thus the truncated boattail is the more efficient of the two, overall, on the basis of aerodynamic drag and useful volume.

REFERENCES

1. Saltzman, E. J. and Meyer, R. R., Jr., "Drag Reduction Obtained by Rounding Vertical Corners on a Box-Shaped Ground Vehicle," NASA TM X-56023, March 1974.
2. Saltzman, E. J., Meyer, R. R., Jr., and Lux, D. P., "Drag Reductions Obtained by Modifying a Box-Shaped Ground Vehicle," NASA TM X-56027, October 1974.
3. Montoya, L. C. and Steers, L. L., "Aerodynamic Drag Reduction Tests on a Full-Scale Tractor-Trailer Combination with Several Add-On Devices," NASA TM X-56028, December 1974.
4. Steers, L. L., Montoya, L. C., and Saltzman, E. J., "Aerodynamic Drag Reduction Tests on a Full-Scale Tractor-Trailer Combination and a Representative Box-Shaped Ground Vehicle," Society of Automotive Engineers, Paper SAE 750703, August 1975.
5. Muirhead, V. U., "An Investigation Of Drag Reduction On Box-Shaped Ground Vehicles," KU-FRL #180, July 1976, The University of Kansas.
6. Hoerner, S. F., "Fluid-Dynamic Drag," published by the author (148 Busteed Dr., Midland Park, N.J.), 1965.
7. White, R. A. and Korst, H. H., "The Determination of Vehicle Drag Contributions from Coast-Down Tests," Society of Automotive Engineers, Paper SAE 720099, January 1972.
8. Korst, H. H. and White, R. A., "Evaluation of Vehicle Drag Parameters From Coast-Down Experiments Conducted Under Non-Ideal Environmental Conditions," Presented at Joint ASME-CSME Applied Mechanics Fluids Engineering and BioEngineering Conference - Niagara Falls, New York, June 18-20, 1979.
9. Dayman, B., Jr., "Effects of Realistic Tire Rolling Resistance upon the Determination of Aerodynamic Drag from Road-Vehicle Coast-Down Tests," Proceedings of the Second AIAA Symposium on Aerodynamics of Sports and Competition Automobiles, Vol. 16, Western Periodicals, Los Angeles, CA , 1975, pp. 229-238.
10. Dayman, B., Jr., "Tire Rolling Resistance Measurements from Coast-Down Tests," Society of Automotive Engineers, Paper SAE 760153, February 1976.
11. Muirhead, V. U., "An Investigation of Drag Reduction for Tractor Trailer Vehicles with Air Deflector and Boattail," NASA CR-163104, January 1981.
12. Muirhead, V. U., "An Investigation of Drag Reduction for a Standard Truck with Various Modifications," NASA CR-163107, May 1981.

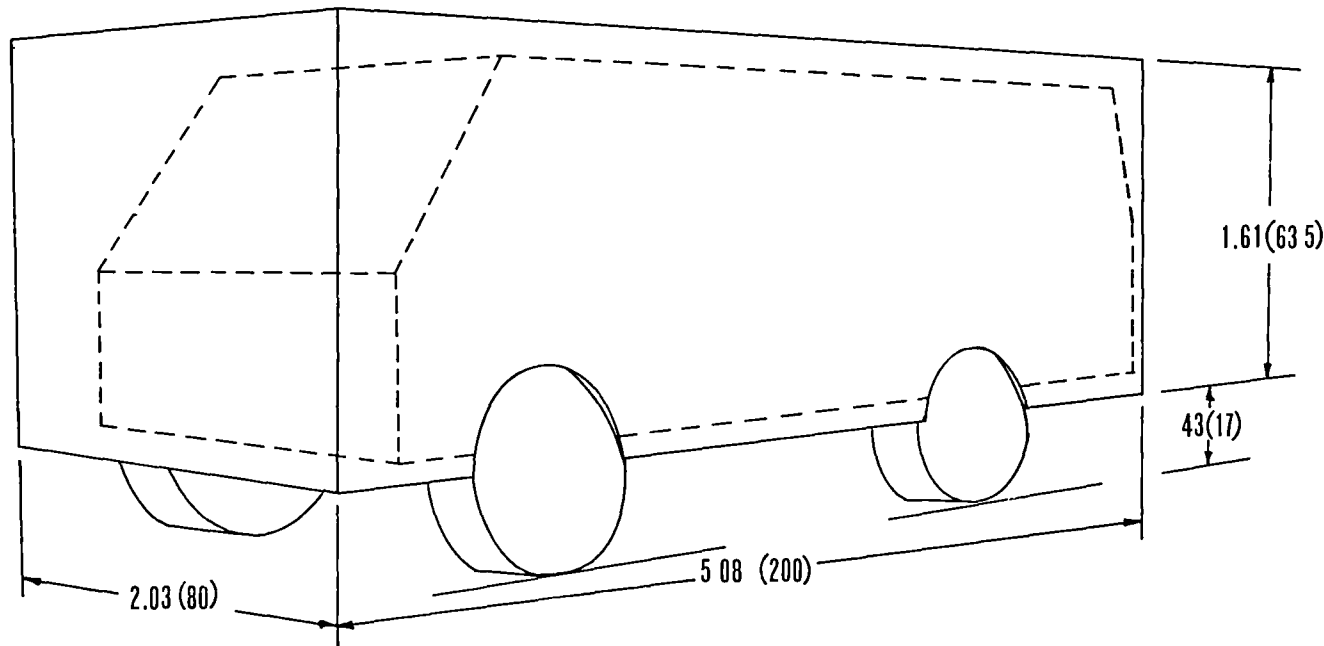
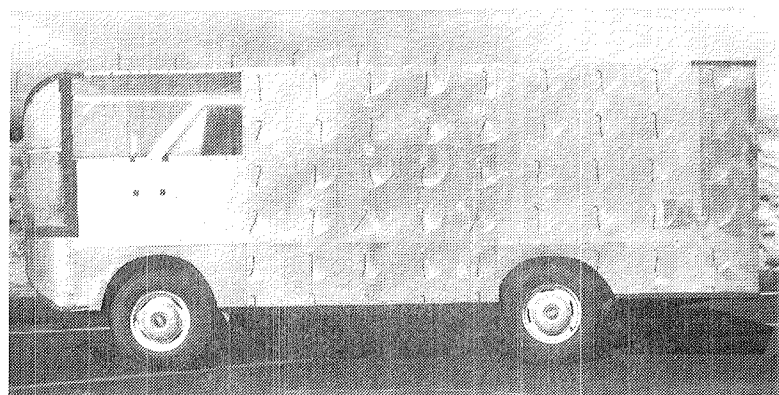
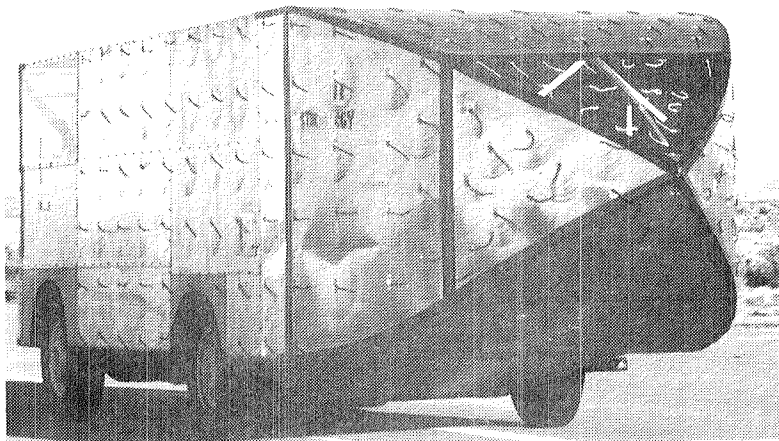


Figure 1. Dimensions of original square-cornered configuration in meters (inches), reference 1



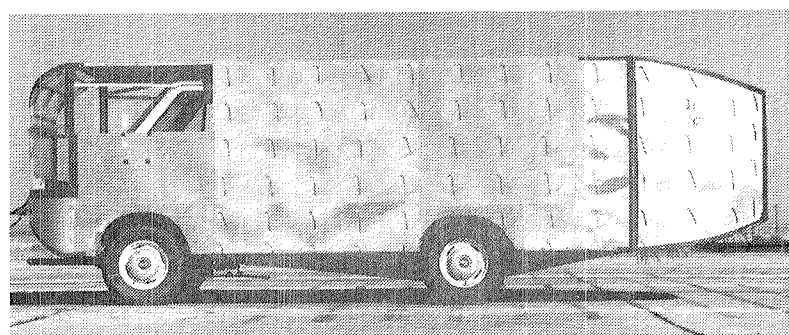
E-38163

Figure 2. Configuration I, $V = 0$ (engine cooling door closed).



E-38011

Figure 3. Configuration II, vehicle in motion.



E-38098

Figure 4. Configuration III, $V = 0$ (engine cooling door open).

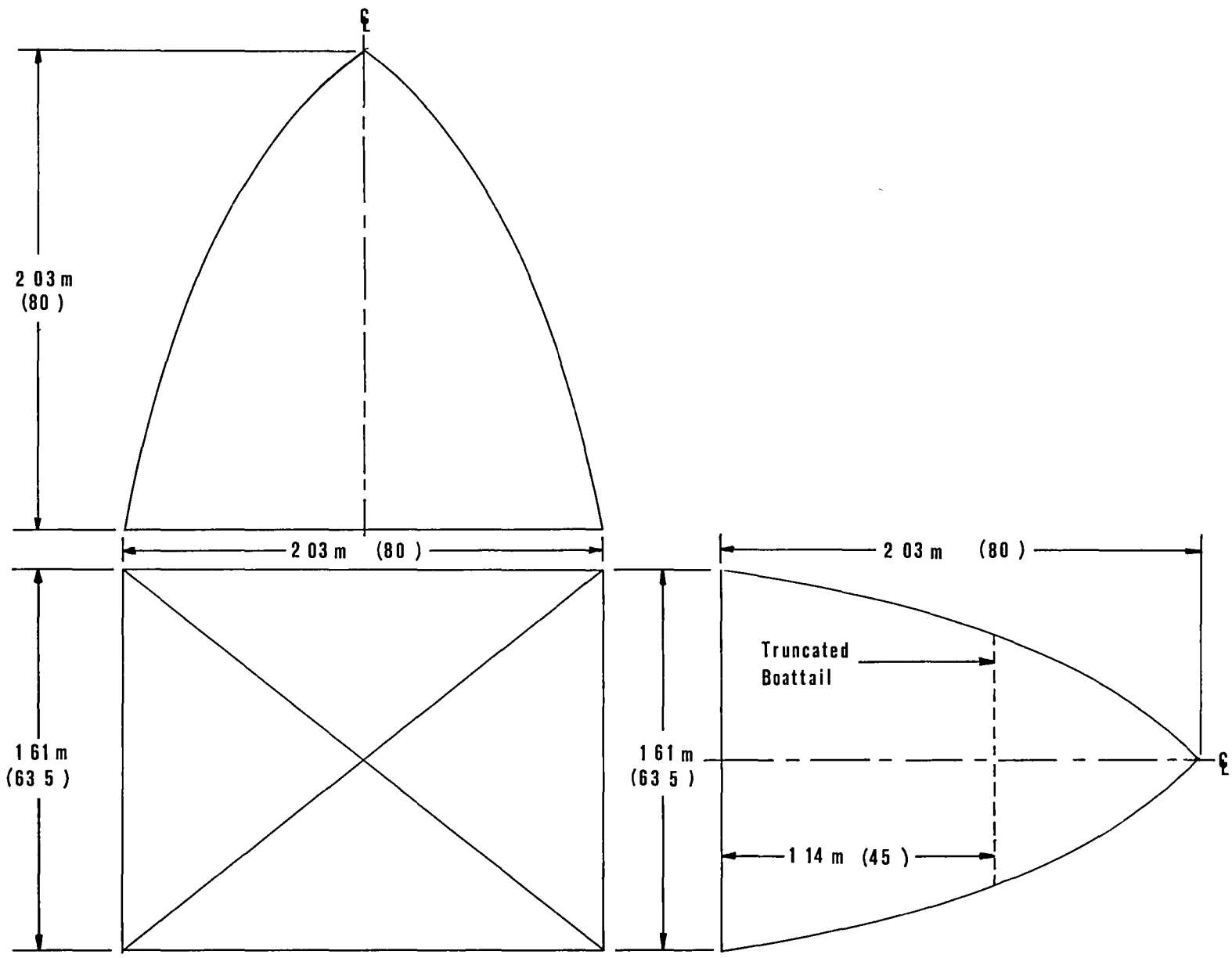
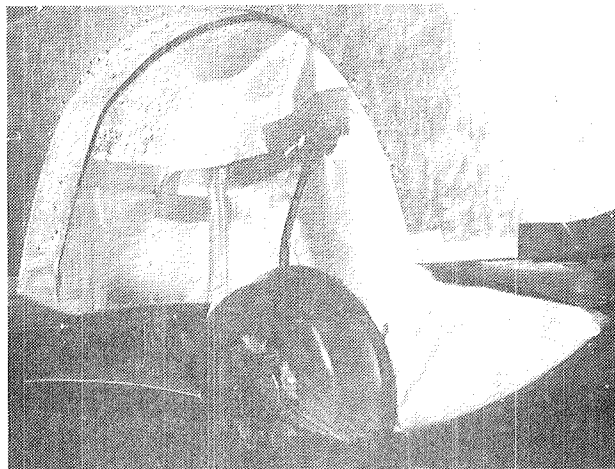
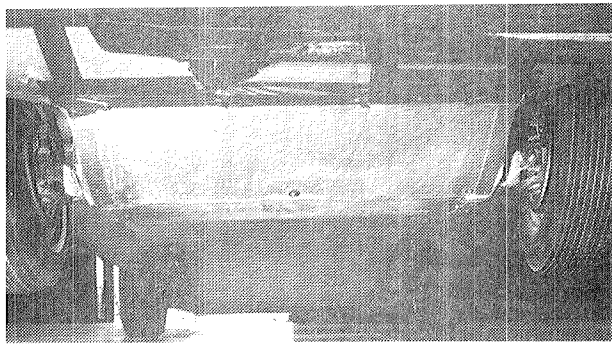


Figure 5. Boattail dimensions.



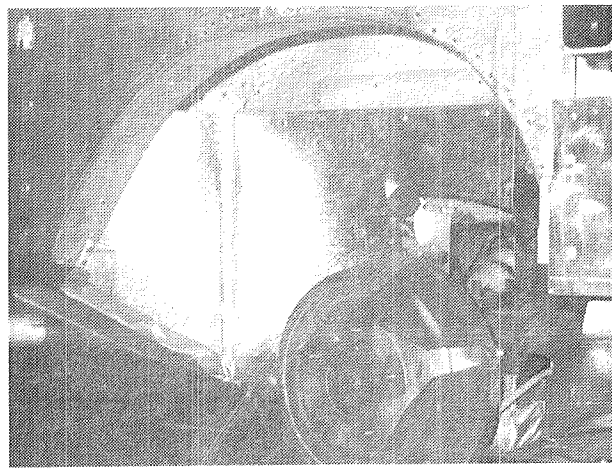
E-37851

Figure 6. Right front wheel well seal as viewed from slightly ahead of wheel station.



E-37848

Figure 7. Sealed underbody as viewed from the front.



E-37854

Figure 8. Right rear wheel well seal as viewed from slightly ahead of axle.

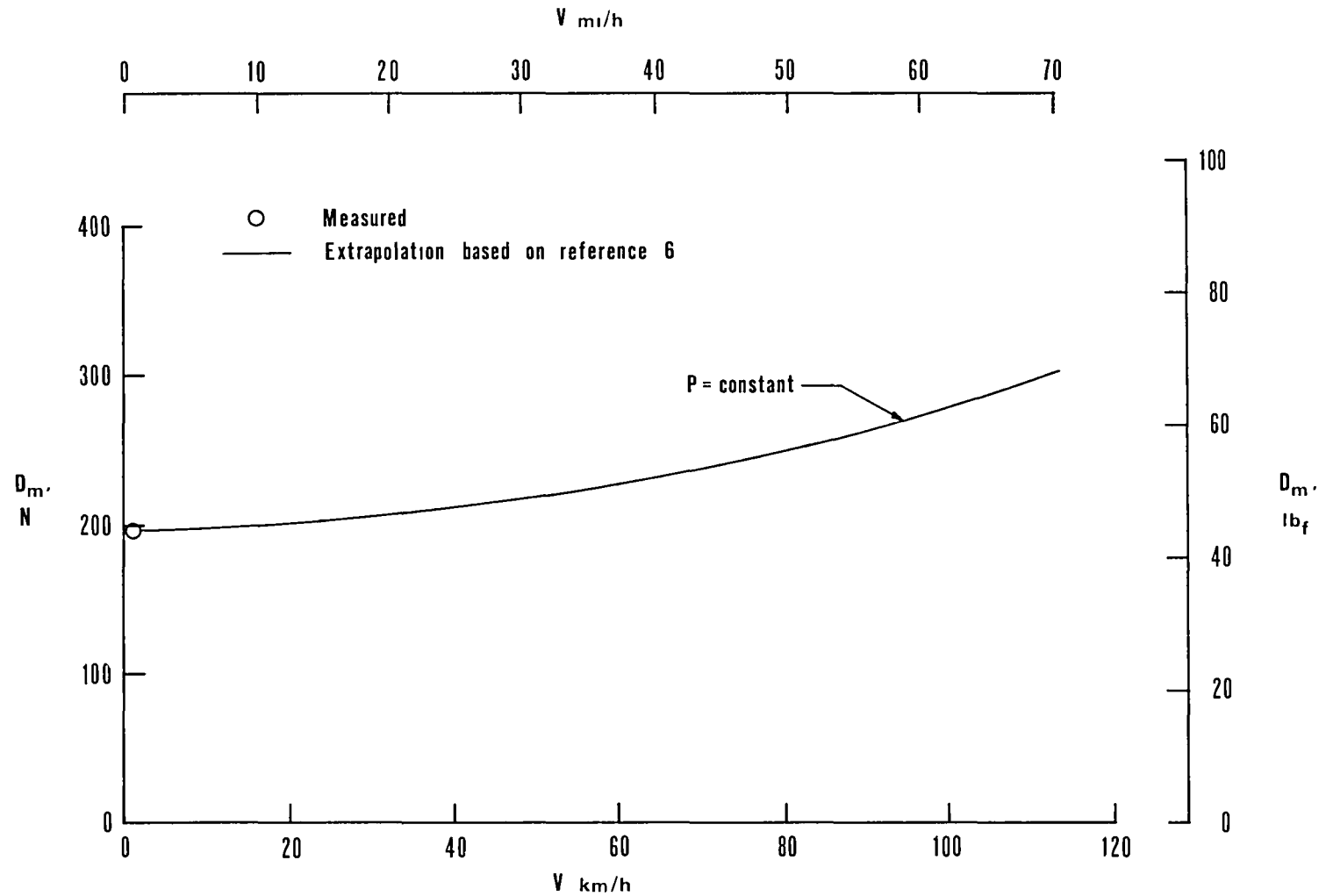
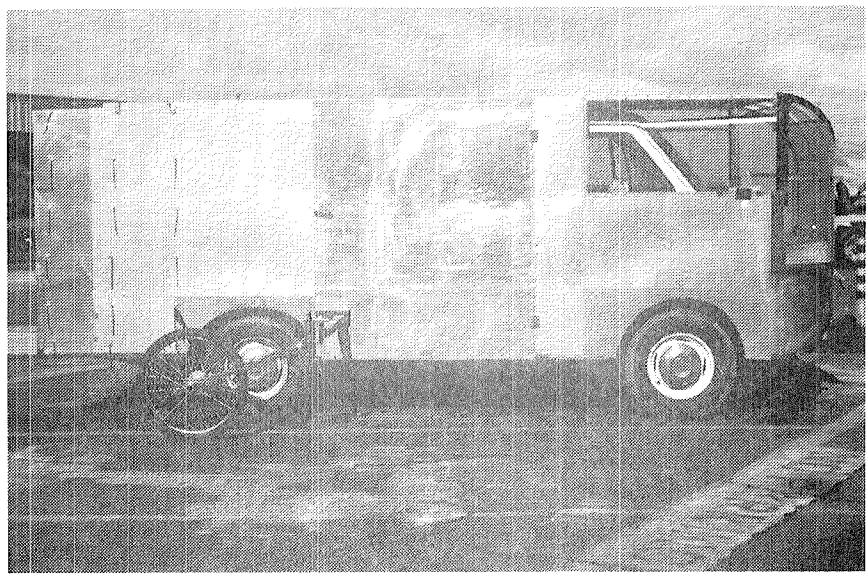
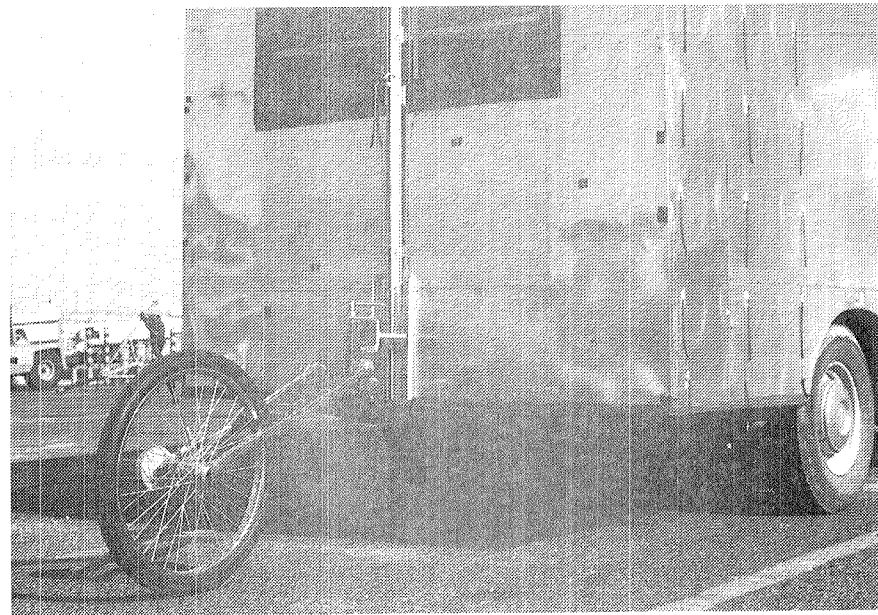


Figure 9 Variation of mechanical drag with vehicle velocity



E-38161

Figure 10. Fifth-wheel and fifth-wheel support system, "side mounting" (configuration I).



E-38158

Figure 11. Fifth-wheel in aft mounting or trailing location (configuration I).

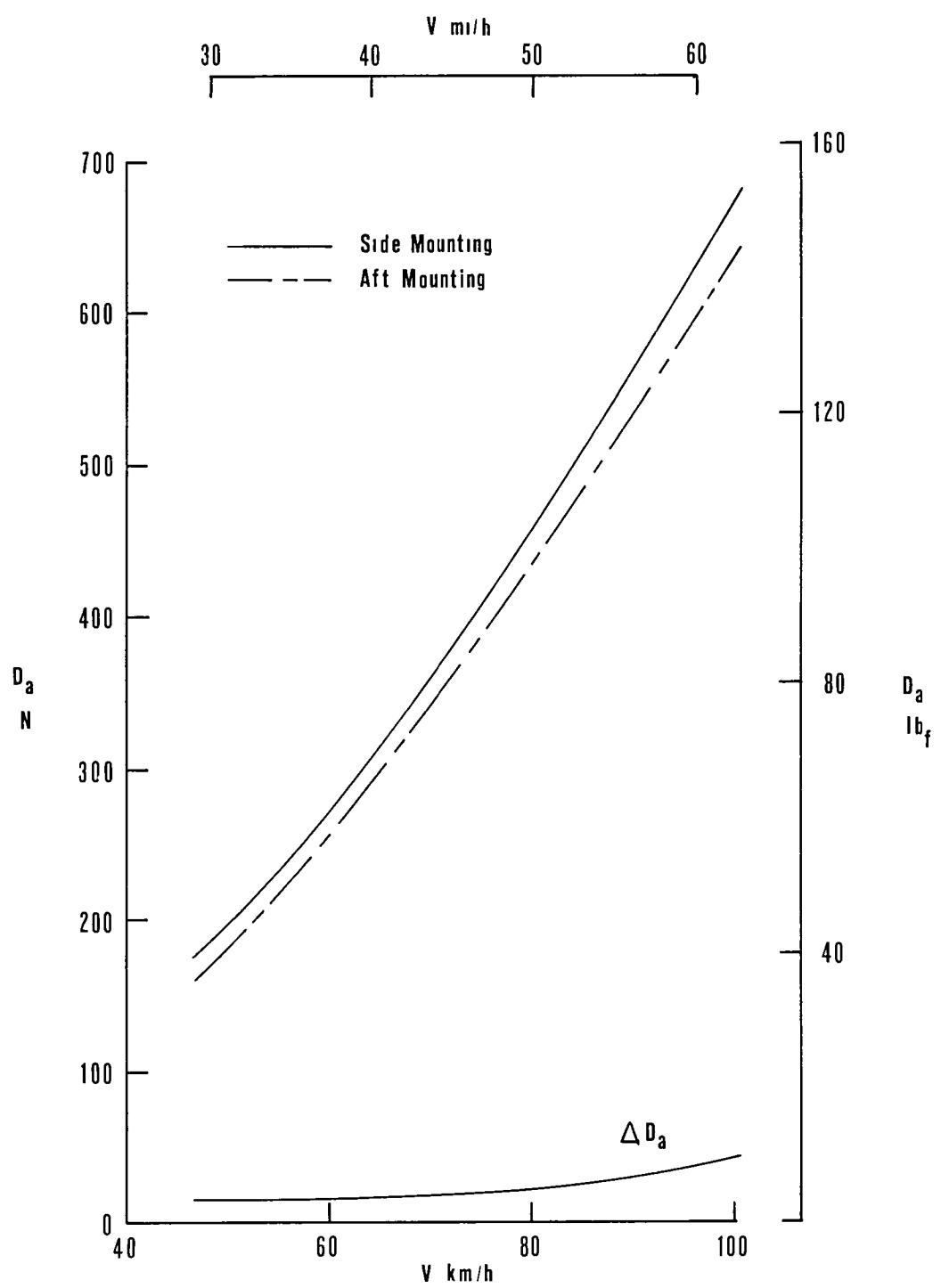
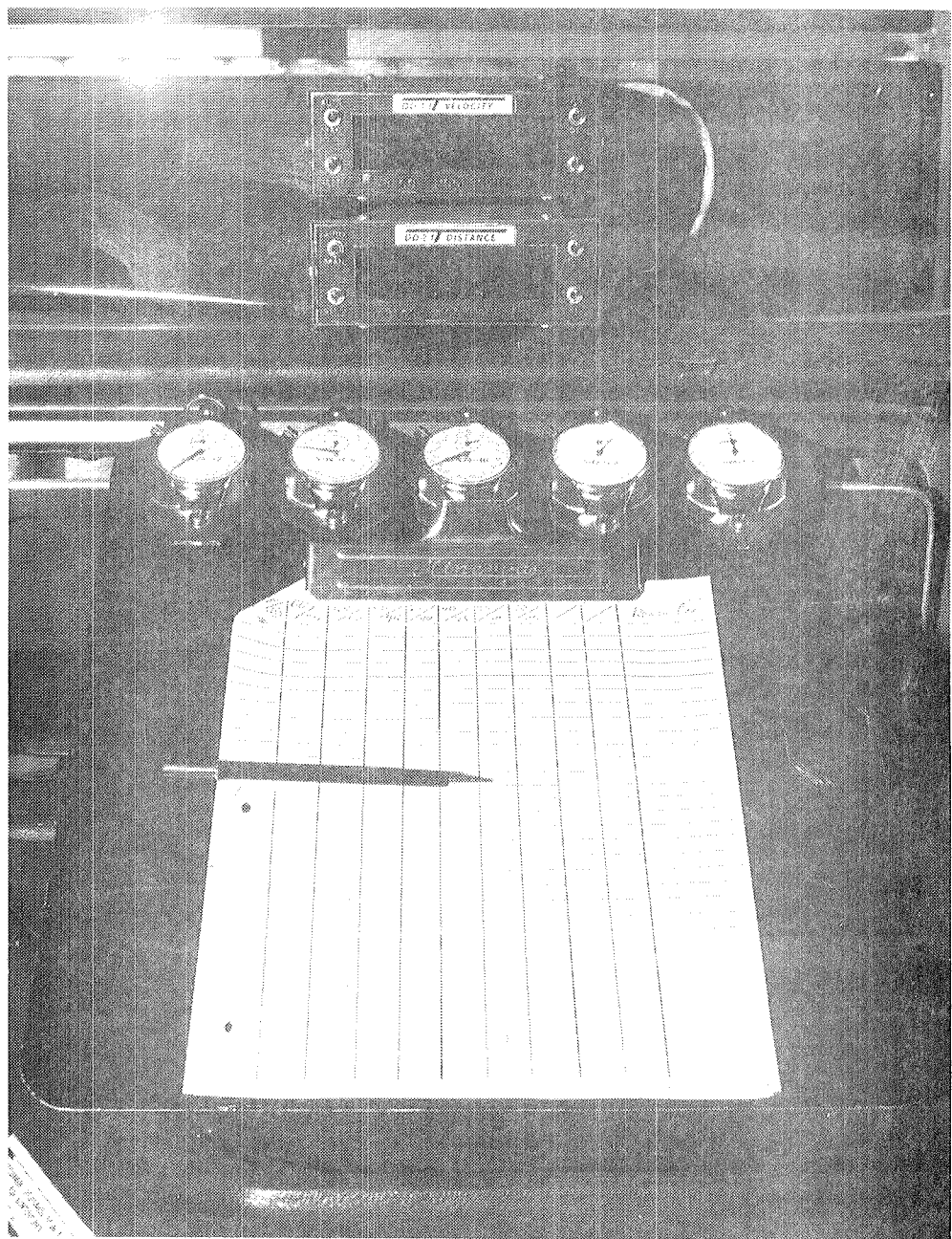
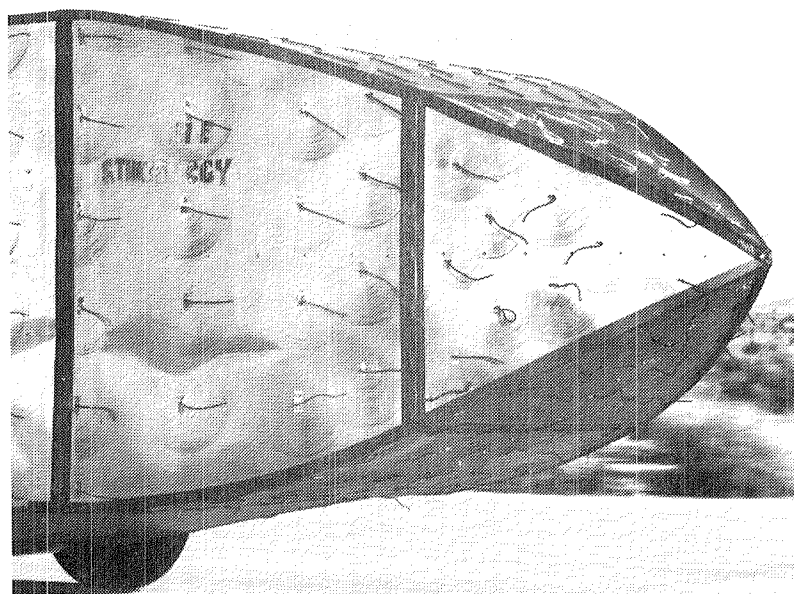


Figure 12 Variation of aerodynamic drag with vehicle velocity for the different fifth-wheel mounting locations, (Configuration I)



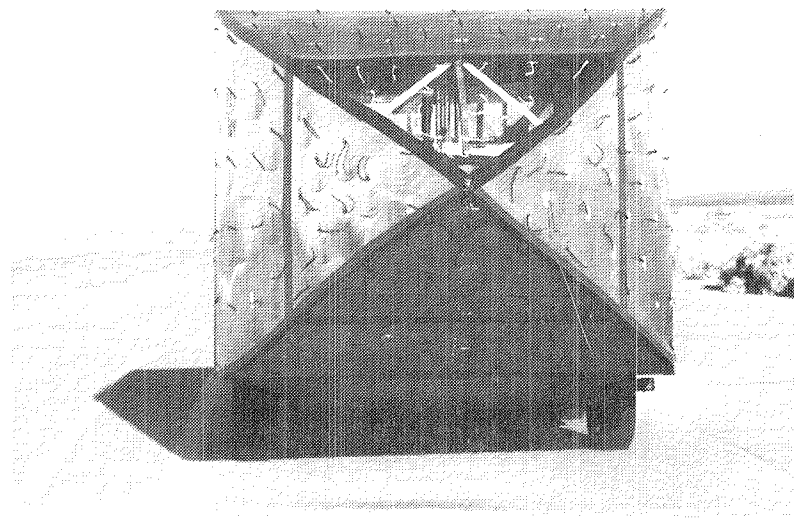
E-38164

Figure 13. Instrumentation layout.



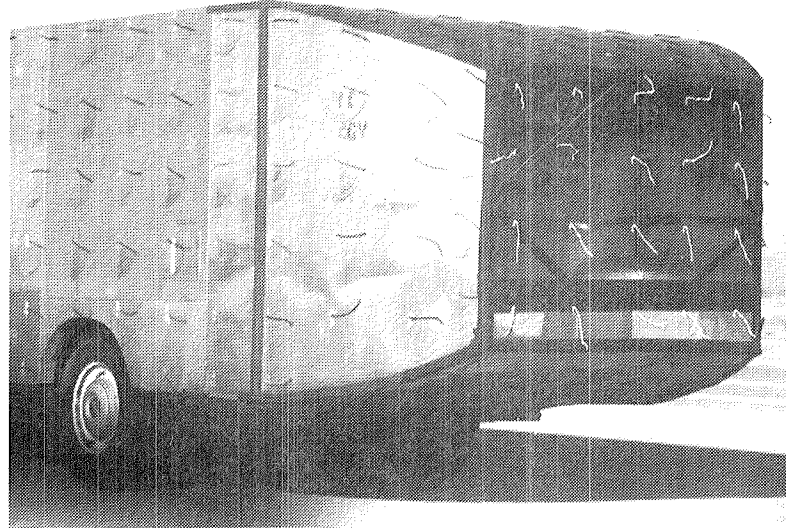
E-38010

Figure 14. Tuft patterns for full boattail, configuration II,
 $V = 116.7 \text{ km/h (72.5 mph)}$.



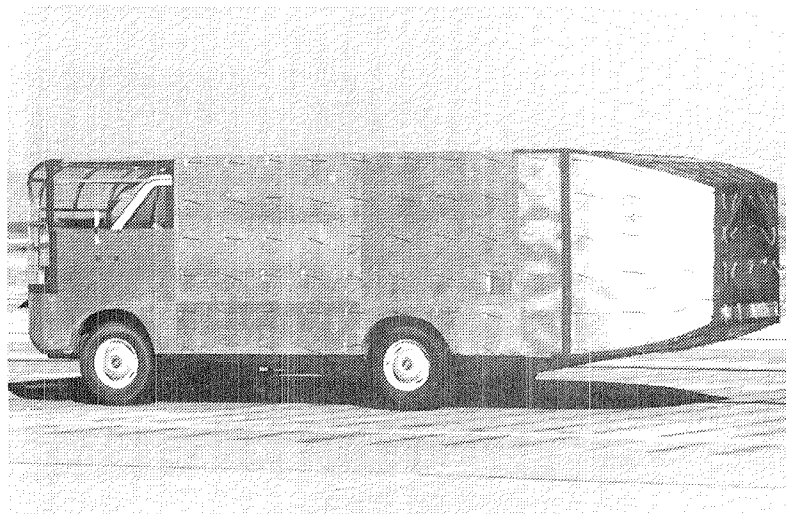
E-38008

Figure 15. Tuft patterns for full boattail, configuration II,
 $V = 116.7 \text{ km/h (72.5 mph)}$.



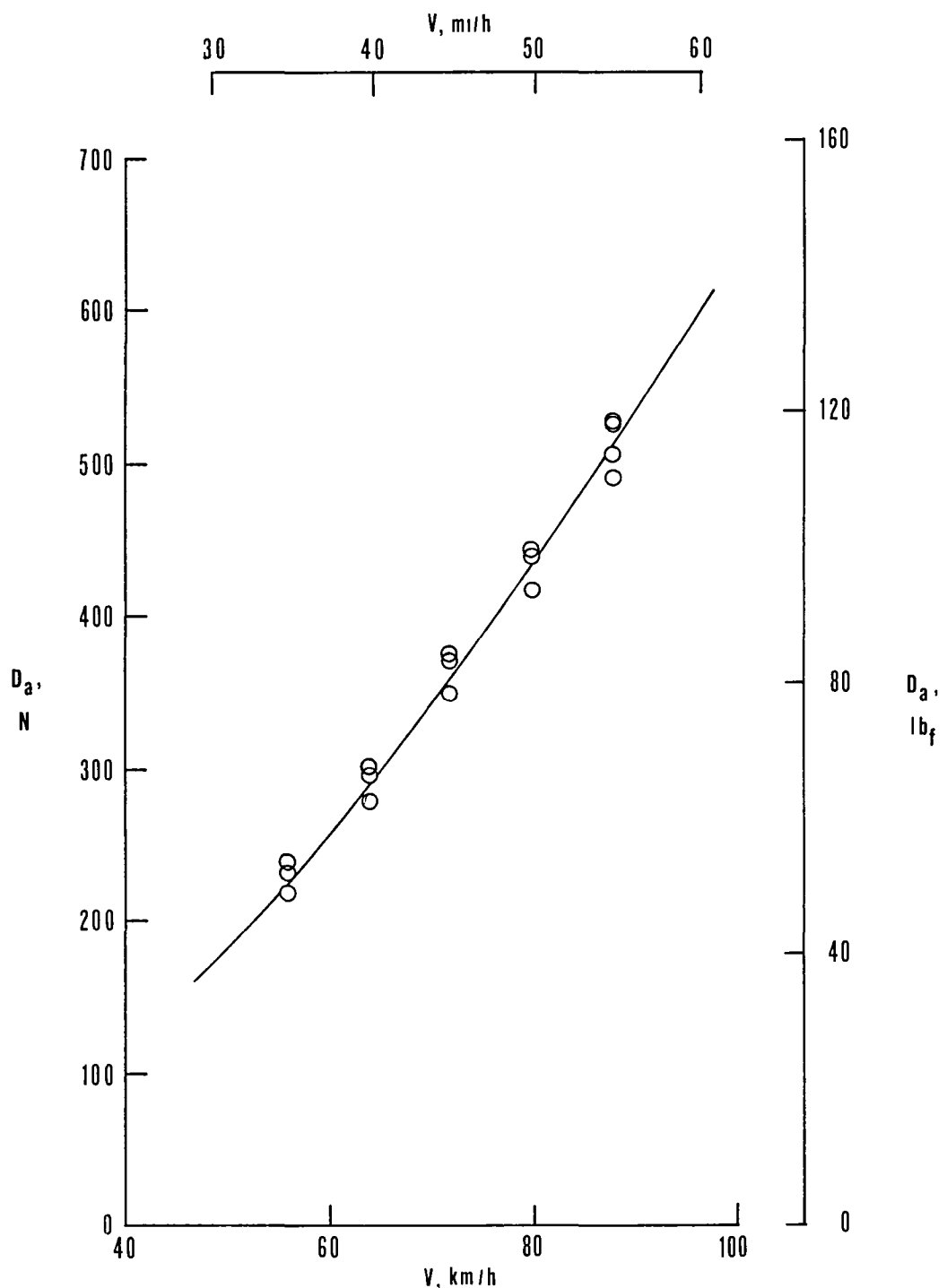
E-38073

Figure 16. Tuft patterns for truncated boattail, configuration III,
 $V = 107.8 \text{ km/h}$ (67 mph) (note "dangling" white tufts
over base region).



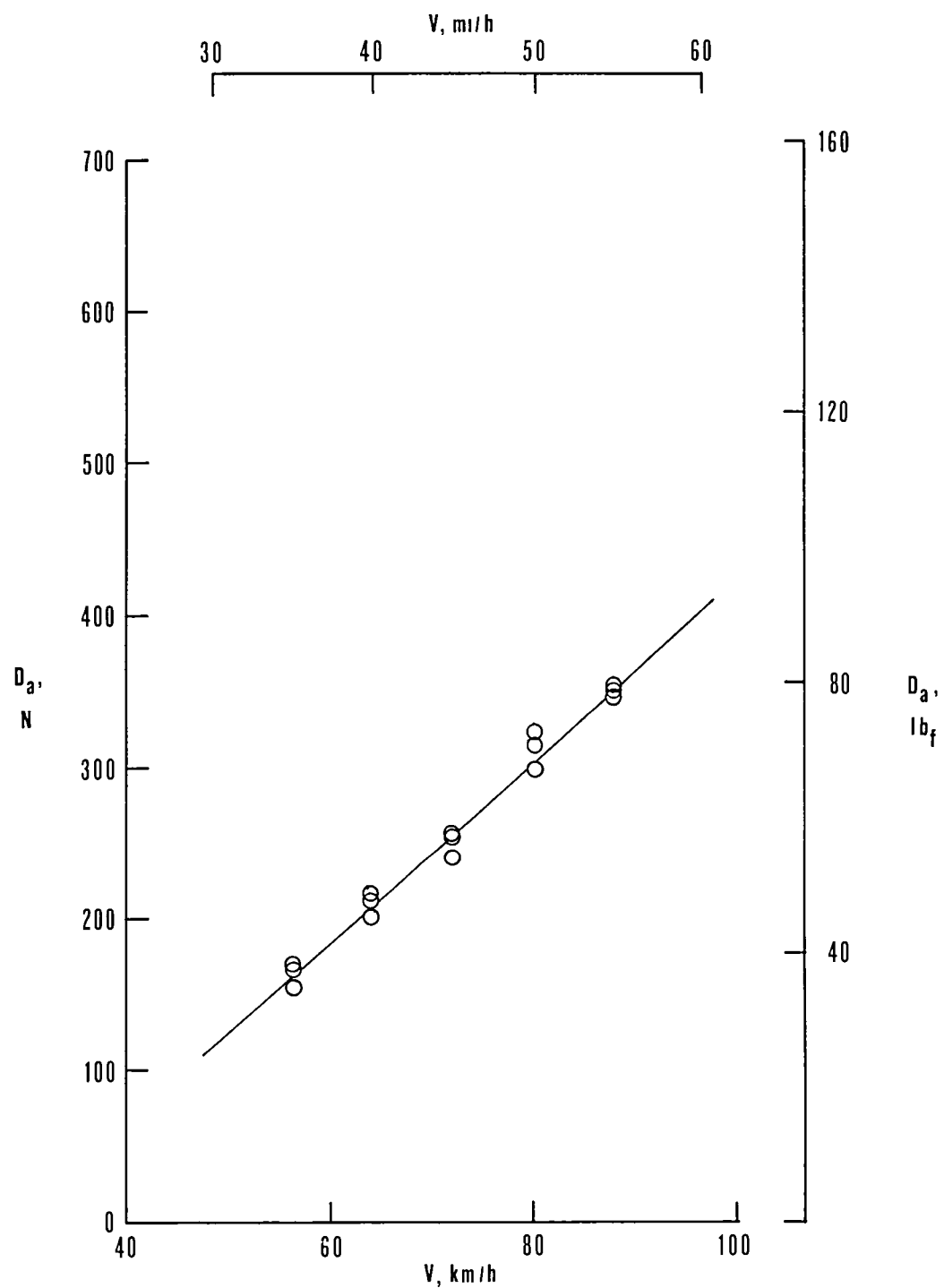
E-38091

Figure 17. Tuft patterns for truncated boattail, configuration III,
 $V = 107.8 \text{ km/h}$ (67 mph) (note "dangling" white tufts
over base region).



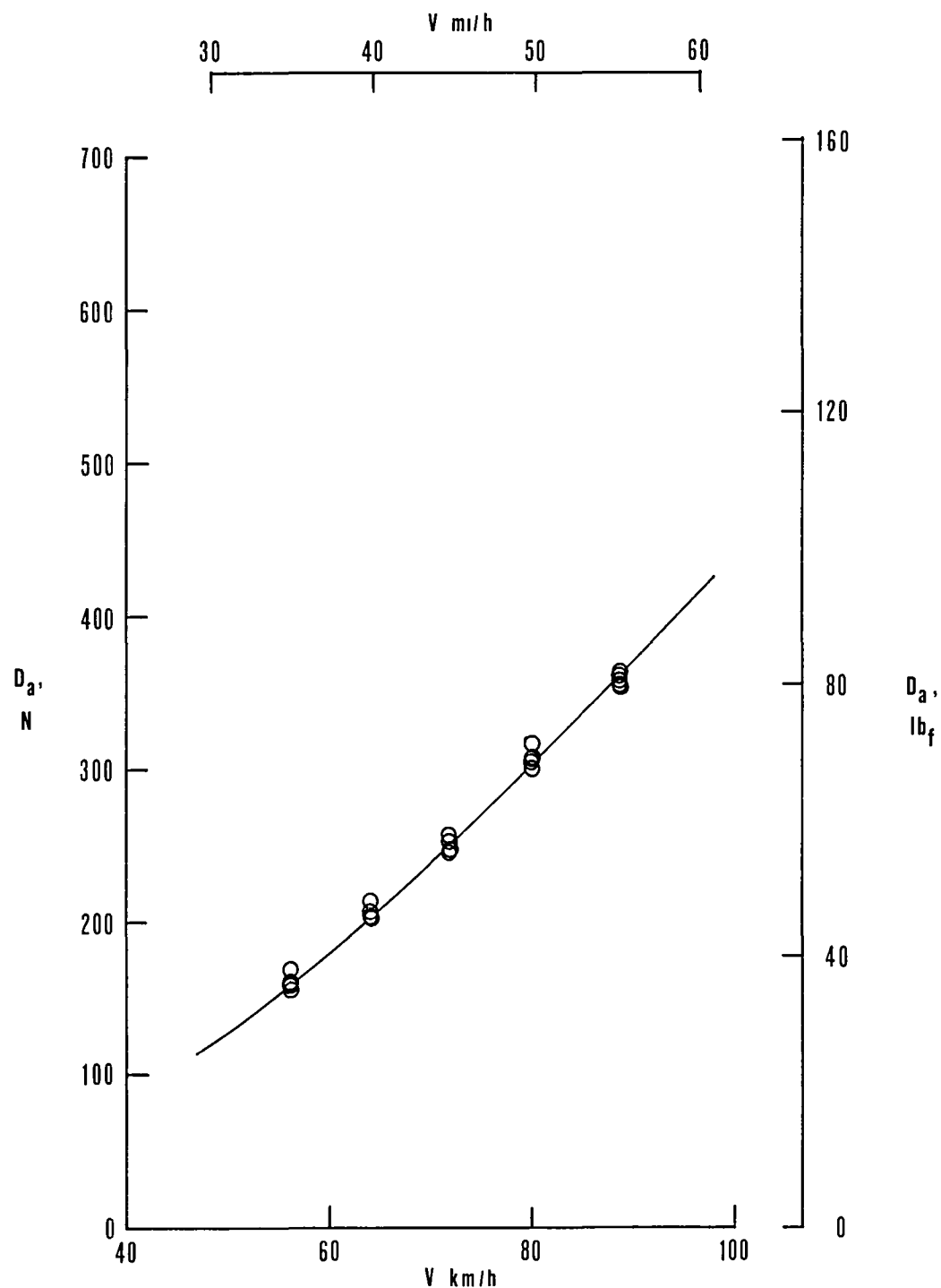
(a) Configuration I, blunt base

Figure 18 Variation of aerodynamic drag with vehicle velocity, drag increment of side mounted fifth-wheel and support system has been removed, (ΔD_a of figure 12)



(b) Configuration II, full boattail

Figure 18 Continued



(c) Configuration III, truncated boattail

Figure 18. Concluded

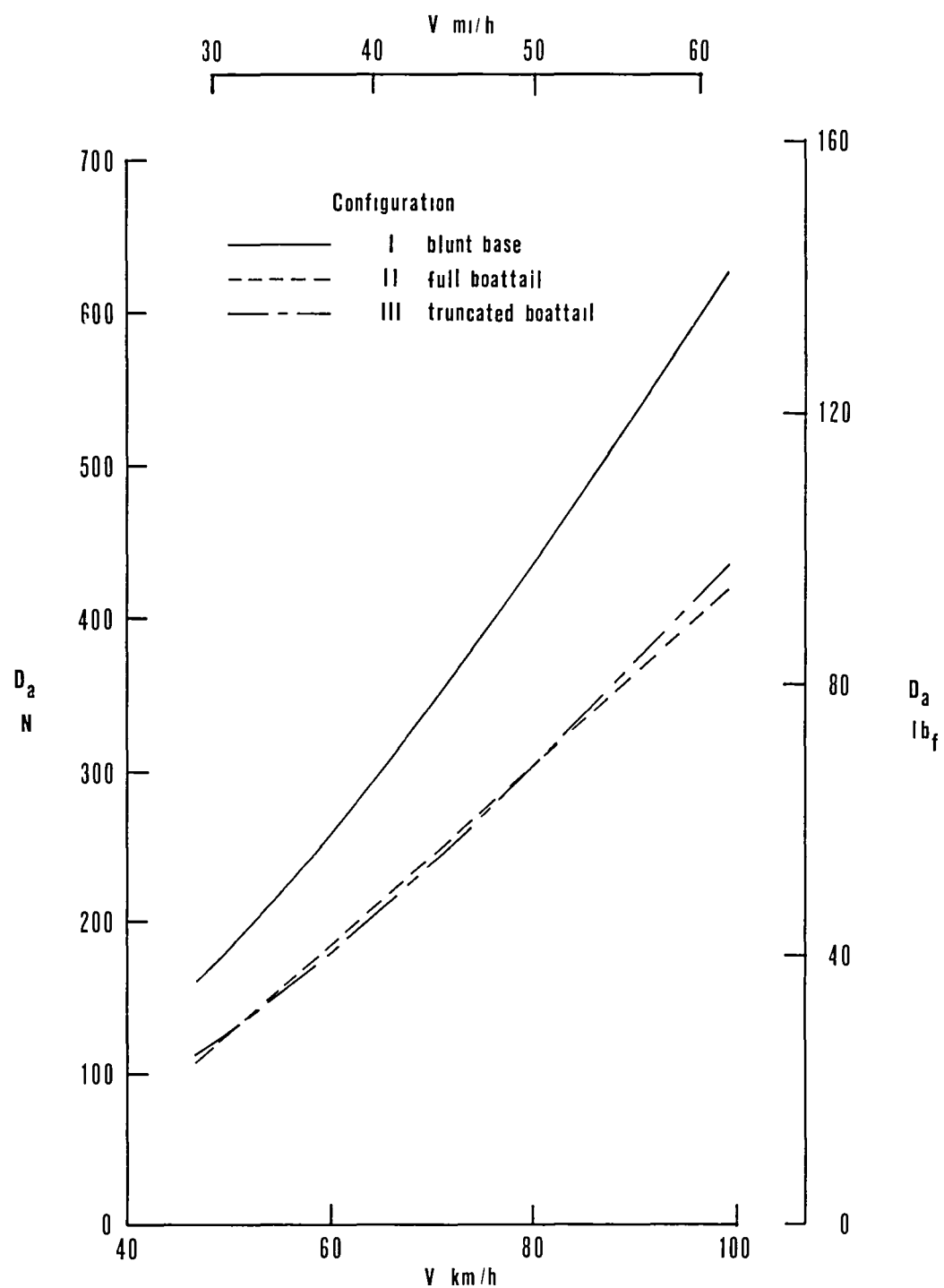


Figure 19 Aerodynamic drag variation with vehicle velocity for all configurations, same data as shown in figure 18

Table I. Comparison of tests run at the Dryden Flight Research Center and the University of Kansas.

Configuration		C_{D_a} , DFRC $R = 1.3 \times 10^7$			C_{D_a} , KU $R = 2.7 \times 10^6$	C_{D_a} , reduction, percent		$\frac{C_{D_a} - C_{D_a}}{DFRC, avg. KU}$
DFRC	KU	80.5 km/h (50 mph)	96.6 km/h (60 mph)	average		DFRC avg	KU	
I	4 14	0.455	0.435	0.445	*(0.426) *0.449 (0.436) 0.459	-	-	-0.9 -3.1
II	16	0.315	0.288	0.302	*(0.270) *0.284	32	37	6.0
III	17	0.314	0.299	0.307	*(0.265) *0.279	31	38	9.1

DFRC = Full-scale tests, Dryden Flight Research Center.

KU = One-tenth scale tests, University of Kansas from reference 5

() = values based on reference area A', as in reference 5

* - these drag coefficients are for configurations without towing hitch, reference 5
(note, full-scale vehicle had towing hitch).

1 Report No NASA CR-163113	2 Government Accession No	3 Recipient's Catalog No	
4 Title and Subtitle DRAG REDUCTION OBTAINED BY THE ADDITION OF A BOATTAIL TO A BOX SHAPED VEHICLE		5 Report Date August 1981	
		6 Performing Organization Code	
7 Author(s) Randall L Peterson		8 Performing Organization Report No	
9 Performing Organization Name and Address California Polytechnic State University San Luis Obispo, CA 93407		10 Work Unit No	
		11 Contract or Grant No NCC 4-1	
12 Sponsoring Agency Name and Address National Aeronautics and Space Administration Washington, D C 20546		13 Type of Report and Period Covered Contractor Report - Topical	
		14 Sponsoring Agency Code RTOP 141-20-11	
15 Supplementary Notes NASA Technical Monitor Edwin J Saltzman, Dryden Flight Research Center This report is substantially the same as the authors masters thesis, which was published under the same title by the Aeronautical-Mechanical Engineering Department of California Polytechnic State University at San Luis Obispo, CA			
16 Abstract Coast-down tests have been performed on a box-shaped ground vehicle used to simulate the aerodynamic drag of high volume transports such as delivery vans, motor homes and trucks. The results of these tests define the reduction in aerodynamic drag that can be obtained by the addition of either a full boattail or a truncated boattail to an otherwise blunt-based vehicle Test velocities ranged up to 96.6 km/h (60 mph) with Reynolds numbers to 1.3×10^7 . The full boattail provided an average 32-percent reduction in drag at "highway speeds" whereas the truncated boattail provided an average 31-percent reduction in drag as compared to the configuration having the blunt base. These results are compared with one-tenth scale wind-tunnel model data			
17 Key Words (Suggested by Author(s)) Aerodynamic drag Streamlining Fuel economy		18 Distribution Statement Unclassified - Unlimited	
19 Security Classif (of this report) Unclassified	20 Security Classif (of this page) Unclassified	21 No of Pages 32	22 Price* A03

*For sale by the National Technical Information Service, Springfield, VA 22161

End of Document